Predicting the Discharge of Global Rivers

BART NIJSSEN, GREG M. O'DONNELL, DENNIS P. LETTENMAIER

University of Washington, Seattle, Washington

DAG LOHMANN* AND ERIC F. WOOD

Princeton University, Princeton, New Jersey

(Manuscript received 25 April 2000, in final form 3 November 2000)

ABSTRACT

The ability to simulate coupled energy and water fluxes over large continental river basins, in particular streamflow, was largely nonexistent a decade ago. Since then, macroscale hydrological models (MHMs) have been developed, which predict such fluxes at continental and subcontinental scales. Because the runoff formulation in MHMs must be parameterized because of the large spatial scale at which they are implemented, some calibration of model parameters is inevitably necessary. However, calibration is a time-consuming process and quickly becomes infeasible when the modeled area or the number of basins increases. A methodology for model parameter transfer is described that limits the number of basins requiring direct calibration. Parameters initially were estimated for nine large river basins. As a first attempt to transfer parameters, the global land area was grouped by climate zone, and model parameters were transferred within zones. The transferred parameters were then used to simulate the water balance in 17 other continental river basins. Although the parameter transfer approach did not reduce the bias and root-mean-square error (rmse) for each individual basin, in aggregate the transferred parameters reduced the relative (monthly) rmse from 121% to 96% and the mean bias from 41% to 36%. Subsequent direct calibration of all basins further reduced the relative rmse to an average of 70% and the bias to 12%. After transferring the parameters globally, the mean annual global runoff increased 9.4% and evapotranspiration decreased by 5.0% in comparison with an earlier global simulation using uncalibrated parameters. On a continental basis, the changes in runoff and evapotranspiration were much larger. A diagnosis of simulation errors for four basins with particularly poor results showed that most of the error was attributable to bias in the Global Precipitation Climatology Project precipitation products used to drive the MHM.

1. Introduction

Macroscale hydrological models (MHMs), which model the land surface hydrologic dynamics of continental-scale river basins, have rapidly developed over the past decade (e.g., Russell and Miller 1990; Kuhl and Miller 1992; Miller et al. 1994; Dümenil and Todini 1992; Sausen et al. 1994; Liston et al. 1994; Abdulla et al. 1996; Nijssen et al. 1997; Wood et al. 1997; Kite 1998). MHMs are closely related to the land surface parameterization schemes (LSPs) in general circulation models, but focus more on modeling of runoff and streamflow and their interaction with other terms in the land surface water budget. They can act as a link between global atmospheric models and water resource systems on large spatial scales and long (seasonal to interannual) timescales (e.g., Hamlet and Lettenmaier 1999).

One practical problem in application of MHMs (and LSPs) is the determination of model parameters. Most MHMs are a hybrid of physically based and conceptual components. The energy exchange at the atmosphere–land surface interface is usually based on physical principles, while the runoff generation mechanisms tend to be more conceptual in nature. For example, the Variable Infiltration Capacity (VIC) model (Liang et al. 1994; Nijssen et al. 1997) uses physically based formulations for the calculation of the sensible and latent heat fluxes, but uses the conceptual ARNO baseflow model (Todini 1996) to simulate runoff generation from the deepest soil layer, and a conceptual scheme to represent the spatial variability in infiltration capacity (Zhao et al. 1980) and hence production of surface runoff. Determination of parameters can therefore be separated into two parts. The parameters for the physically based part of the model can, in principle, be determined through direct observation. In practice, given the large areas over which MHMs are applied, this is a challenge. Most mod-

* Current affiliation: National Centers for Environmental Predictions, Camps Springs, Maryland.

Corresponding author address: Dennis P. Lettenmaier, Department of Civil and Environmental Engineering, Box 352700, University of Washington, Seattle, WA 98195-2700.
E-mail: dennisl@u.washington.edu

© 2001 American Meteorological Society

els use some form of lookup-table approach in which land surface attributes are kept constant within each land surface class, and vary only between different classes. This simplifies the application and greatly reduces the number of parameters that need to be specified.

It is less obvious whether or how the parameters for the conceptual parts of the model can be specified a priori. Traditionally, conceptual hydrological models are tailored to a specific application through a process of calibration (e.g., Linsley et al. 1986, chapter 12). In this process model parameters are adjusted in successive model simulations until the model output matches observations to within a previously determined error criterium. Although this is a relatively straightforward process for a small river basin, the approach tends to be piecemeal and labor intensive for large river basins. For example, application of the National Weather Service River Forecast System to the Columbia River in the Pacific Northwest required calibration of the model to over 100 subbasins (Riverside Technologies, Inc., Harza Engineering 1994).

The Project for Intercomparison of Land surface Parameterization Schemes (PILPS) Phase 2(c) (Wood et al. 1998) was designed to provide some insight into the effects of calibration on MHMs and LSPs applied over a large river basin. PILPS 2(c) evaluated the ability of 16 models run in offline mode to reproduce observed water and energy fluxes over the Arkansas–Red River basin in the Southern Great Plains region of the United States (Liang et al. 1998; Lohmann et al. 1998c). The runoff produced by each of the 16 models was then routed to the basin outlets using the routing model of Lohmann et al. (1998a) as a postprocessor. As part of PILPS 2(c), the effect of calibration on simulated streamflow was studied for 11 of the 16 participating LSPs (Wood et al. 1998). Selected parameters of each model were calibrated (by the model developer) for a number of small basins, and subsequently the parameters were transferred to the entire Arkansas–Red River basin, which consisted of 61 $1° \times 1°$ model grid cells. A set of ''verification basins,'' of similar size to those used for calibration, was used in a blind experiment to determine the effects of calibration on model performance. It was left to the participants to choose the method for transferring the model parameters. A key result of PILPS 2(c) was that model performance improved significantly for those models that were able to use streamflow information effectively for model calibration. Model performance for the validation catchments was generally much better for those models that calibrated than for those that did not. Consequently, Wood et al. (1998) suggested that there is value in using catchment data to calibrate the parameters of land surface schemes, even for so-called physically based models, whose parameter values, in theory, can be obtained through direct observation. Early work on the transfer of calibrated model parameters from small calibration catchments to continental-scale river basins by Abdulla and Lettenmaier (1997a,b) has demonstrated the potential for such approaches in continental hydrology. The results from these two studies provide the motivation for the current work.

2. Objectives and modeling strategy

The objectives of this paper are twofold. The first objective is to evaluate the change in model performance achieved when a simple parameter transfer method is used, based on model calibration for a limited number of large river basins. The second objective is to provide a dataset of global runoff estimates and accompanying components of the land surface hydrological cycle, such as evapotranspiration, soil moisture storage, and snow water equivalent. The resulting dataset can be used in large-scale water management studies, or as a benchmark for comparison with runoff estimates from large-scale climate simulations in which the land surface hydrology is forced with model meteorology (e.g., Maurer et al. 2001).

The model setup, model parameters, and meteorological forcing dataset from Nijssen et al. (2001) were taken as the starting point for this study. Nijssen et al. (2001) simulated the global, land surface hydrological cycle based on observed meteorological forcings at a $2° \times 2°$ resolution for the period 1979–93, using the VIC model. No calibration was performed in that study.

The selection of continental-scale river basins used in this study was based on the dataset from Graham et al. (1999) as modified by Comanor et al. (2000). To assess the effects of calibration and parameter transfer, the selected basins were partitioned into two groups. The basins in the first set (primary basins) were calibrated using an approach described in section 5. The primary basins represent a range of climate and vegetation types. Calibration focused on matching observed and simulated streamflow. Streamflow is arguably the most easily measured and best documented component of the regional surface water balance. It acts as an integrator of the runoff response from all parts of a river basin. As such, streamflow offers the opportunity to verify the surface water balance simulated by MHMs. Other model-predicted water storage and flux components (e.g., soil water storage, snow cover, evapotranspiration) are rarely observed at spatial and temporal scales suitable for direct comparison with the output from MHMs. Some observational soil moisture datasets exist, which have been used for comparison with GCMs and macroscale hydrological simulations (e.g., Robock et al. 1998, 2000), but both their temporal and spatial extent are limited. On the other hand, streamflow is available for many major rivers, often for extended periods of time. We do, however, show later in this paper that even streamflow observations are often not readily available for many global rivers for the period since 1984.

Basins in the second set (secondary basins) were ini-

tially modeled using parameters transferred from the calibrated primary basins using the parameter transfer method described in section 5. Observed and simulated streamflow for these basins were compared to determine the effectiveness of the parameter transfer method.

The secondary basins were then calibrated in a second stage of the study. This second stage served two purposes. First, calibration of the secondary basins served to further evaluate the effectiveness of the parameter transfer process. Ideally, this calibration should result in minimal improvement of model results, which would indicate that the parameter transfer process was highly successful. Second, the second stage calibration ensured that the global estimates of water balance components were the best possible, given the model and meteorological forcings. In a final step, the calibrated parameters from all basins were transferred to the remaining global land surface grid cells to allow estimation of the continental and global water balance.

3. Model implementation and data sources

The VIC model (e.g., Liang et al. 1994, 1996) is an MHM that has been used in a number of modeling studies of large river basins (e.g., Abdulla et al. 1996; Bowling et al. 2000; Lohmann et al. 1998b; Maurer et al. 2000; Nijssen et al. 2001, 1997; Wood et al. 1997). Distinguishing characteristics of the VIC model include the representation of the following:

- subgrid variability in land surface vegetation classes;
- subgrid variability in the soil moisture storage capacity, which is represented as a spatial probability distribution;
- drainage from the lower soil moisture zone (baseflow) as a nonlinear recession;
- spatial subgrid variability in precipitation.

Results from previous work by Nijssen et al. (2001) were used as the starting point for the current study. In Nijssen et al. (2001) a gridded dataset of daily meteorological model forcings for the period 1979–93 was developed for global land areas (excluding Greenland and Antarctica) at a spatial resolution of $2° \times 2°$. This dataset was then used to drive the VIC model to calculate a set of derived variables (evapotranspiration, runoff, snow water equivalent, and soil moisture) and to study the water balance of each of the continents. One specific purpose of the study was to develop global soil moisture fields constrained by observed meteorological forcings. Although the reader is referred to Nijssen et al. (2001) for details regarding the development of the dataset, a very brief overview is given here.

In Nijssen et al. (2001), daily precipitation and daily minimum and maximum temperatures were derived from station observations, and extended using stochastic interpolation methods for those areas where not enough daily meteorological stations were available. The resulting daily sequences were scaled to match the means of existing global, monthly time series (Hulme 1995; Huffman et al. 1997; Jones 1994). Daily surface wind speeds were obtained from the National Centers for Environmental Prediction–National Center for Atmospheric Research reanalysis project (Kalnay et al. 1996). The remaining meteorological forcings (vapor pressure, incoming shortwave radiation, and net longwave radiation) were calculated based on daily temperature and precipitation using algorithms by Kimball et al. (1997), Thornton and Running (1999), and Bras (1990).

For each $2° \times 2°$ model grid cell land surface characteristics such as elevation, soil, and vegetation were specified. Elevation data were calculated based on the 5-min TerrainBase Digital Elevation Model (Row et al. 1995), using the land surface mask from Graham et al. (1999). Vegetation types were provided by the Advanced Very High Resolution Radiometer–based, 1-km, global land classification from Hansen et al. (2000), which has 12 unique vegetation classes. Vegetation parameters such as height and minimum stomatal resistance were assigned to each individual vegetation class. Soil textural information and soil bulk densities were derived from the 5-min Food and Agricultural Organization (FAO)–United Nations Educational, Scientific, and Cultural Organization digital soil map of the world (FAO 1995), combined with the World Inventory of Soil Emission Potentials pedon database (Batjes 1995). The remaining soil characteristics, such as porosity, saturated hydraulic conductivity, and the exponent for the unsaturated hydraulic conductivity equation were based on Cosby et al. (1984).

In Nijssen et al. (2001), the soil depth was set at 1 m for all grid cells, with an upper horizon of 0.3 m and a lower horizon of 0.7 m. In addition a deeper layer without roots was specified, from which baseflow was generated using the ARNO baseflow formulation (Todini 1996). This layer had a water storage capacity of 100 mm, corresponding to a depth of about 0.25 m, depending on the porosity.

Comparison with previous estimates of the global and continental water balance showed that the components of the water balance (precipitation, evapotranspiration, and runoff), were similar to those earlier estimates, but that runoff was somewhat lower for some of the continents, especially South America.

4. Runoff production and flow routing

a. Data sources

River basins were delineated based on Graham et al. (1999) as corrected by Comanor et al. (2000). This dataset provides river basin outlines at 5-min resolution for 55 major river basins. The resulting 5-min masks and flow accumulation files were aggregated to $1° \times 1°$ routing networks using the algorithm of O'Donnell et al. (1999), which results in routing networks similar to those produced by Oki and Sud (1998). However, the

O'Donnell et al. algorithm allows for automatic extraction of coarser-resolution networks from high-resolution flow accumulation files, so that in principle the model output could be routed at any grid resolution supported by global digital elevation data.

River discharge records were obtained from the Global River Discharge Center (GRDC) in Koblenz, Germany, and from the RivDis 1.1 database (Vörösmarty et al. 1998), both of which provide historical monthly river discharge values globally. Daily discharge data from GRDC were used for the derivation of the ARNO baseflow parameters as discussed in the appendix.

b. Flow routing

The VIC model calculates the daily baseflow and ''fast response'' flow that are generated within each grid cell. A stand-alone routing model is then used to route these flows downstream. The routing model is described in detail by Lohmann et al. (1996, 1998a). Flow can exit each grid cell in eight directions and all flow must exit in the same direction. The flow from each grid cell is weighted by the fraction of the grid cell that lies within the basin.

Once the water is in the routing network it is effectively removed from the surface hydrological cycle. The routing model does not account for flood plain–channel interaction, evaporation from the channel, or loss of river water through infiltration in the river bed. As pointed out by Kite (1998), this is problematic in those regions where these phenomena significantly affect the river discharge. For example, observed flows on the Niger River in West Africa decrease from about 1540 $m^3\ s^{-1}$ to 1140 $m^3\ s^{-1}$ between Koulikoro, Mali, and Gaya, Niger, even though the upstream area is $1.2 \times 10^5\ km^2$ at Koulikoro and almost 10 times larger ($1.0 \times 10^6\ km^2$) at Gaya. The processes responsible for these channel losses are not represented by the routing model.

Similarly, the routing model does not account for extractions, diversions, or reservoir operations. Consequently, the simulated flows are natural flows and cannot be compared directly to measured river discharges on heavily regulated rivers. However, the generated stream discharges can be used as input to reservoir and water resources model (e.g., Hamlet and Lettenmaier 1999; Leung et al. 1999).

For this application the flows were routed on a $1° \times 1°$ network. The four $1° \times 1°$ flow cells within each $2° \times 2°$ VIC model cell were assigned the same daily runoff values. The higher-resolution flow networks allowed a somewhat better approximation of the modeled flow network to the main stem river.

c. Selected rivers

Because observed streamflows were used for calibration, and because the routing model does not account for water resources developments on the river, river basins were selected using the following criteria:

- observed monthly flows had to be available for at least part of the period 1980–93;
- rivers had to be only minimally affected by extractions, diversions, and dams;
- the selected river basins had to cover a variety of climatic regions and continents.

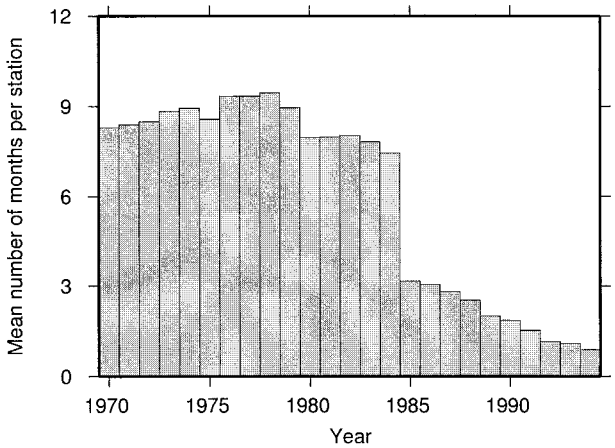

FIG. 1. Total number of nonmissing monthly flow observations in either the RivDis or GRDC database for each year from 1970 to 1994 at a downstream gauge location on each of the 55 rivers in Graham et al. (1999). The data represent the gauge used in this study, or the most downstream gauge available.

Following these criteria, nine rivers were excluded because of significant flow regulation. The reservoir storage on each of these rivers was greater than the mean annual runoff volume. A further 20 rivers were excluded because of insufficient flow records coincident with the analysis period or similar problems. Although the GRDC and/or RivDis databases contain flow records for all except 4 of the original 55 river basins, the number of available records decreases rapidly after 1984 (Fig. 1).

Table 1 lists the 26 selected rivers (see also Fig. 2), with the categories as described in section 5. Not surprisingly, the final group of rivers overrepresents the colder climates. Generally, more complete streamflow records are available in these areas and reservoir storage is less important than in warmer, drier climates (Vörösmarty et al. 1997).

5. Calibration and parameter transfer

Only a limited number of model parameters were targeted for calibration. The variable infiltration parameter (b_i) controls the amount of water that can infiltrate into the soil as a function of soil moisture. Although Dümenil and Todini (1992) assert that the variable infiltration parameter is a function of the topographical properties of the terrain within a model grid cell, Wood et al. (1992)

TABLE 1. Selected river basins.

River basin	Gauge location	Predominant climatic zones	Area (km^2) upstream of gauge*
		Category 1**	
Amazon	Obidos, Brazil	Tropical	4 618 746
Congo	Brazzaville, Congo	Tropical	3 475 000
Danube	Drobeta-Turnu Severin, Romania	Midlatitude rainy	576 232
MacKenzie	Normal Wells, Canada	Arctic	1 570 000
Mekong	Pakse, Laos	Tropical	545 000
Mississippi	Vicksburg, United States	Midlatitude rainy	2 964 254
Senegal	Bakel, Senegal	Arid hot Tropical	218 000
Yellow	Yuayuankou, China	Arid cold Midlatitude rainy	730 036
Yenisei	Igarka, Russia	Arctic	2 440 000
		Category 2**	
Amur	Komsomolsk, Russia	Arctic Midlatitude rainy	1 730 000
Brahmaputra	Bahadurabad, Bangladesh	Midlatitude rainy Arid cold	636 130
Changjiang	Datong, China	Midlatitude rainy	1 705 383
Columbia	The Dalles, United States	Midlatitude rainy	690 000
Indigirka	Vorontsovo, Russia	Arctic	305 000
Irrawaddy	Sagaing, Myanmar	Midlatitude rainy	117 900
Kolyma	Srednekolymsk, Russia	Arctic	361 000
Lena	Kusur, Russia	Arctic	2 430 000
Ob	Salekhard, Russia	Arctic	2 430 000
Olenek	Downstream of Pur River, Russia	Arctic	198 000
Paraná	Corrientes, Argentina	Midlatitude rainy	2 300 000
Pechora	Ust-Tsilma, Russia	Arctic	248 000
Severnaya Dvina	Ust-Pinega, Russia	Arctic	348 000
Volga	Volgograd, Russia	Midlatitude rainy	1 360 000
Xi	Wuzhou, China	Midlatitude rainy	329 705
Yana	Dzhangky, Russia	Arctic	216 000
Yukon	Ruby, United States	Arctic	670 810

* Areas are taken from the GRDC and RivDis databases.

** As explained in section 2, category-1 rivers are used in the first round of calibration, and category-2 rivers are used in the second round of calibration.

argue that this parameter must be determined through calibration. The remaining calibration parameters, namely, the depth of the second soil layer (D_2), the saturated hydraulic conductivities of the first and second layers (k_{s_1} and k_{s_2}), and the exponents for the unsaturated hydraulic conductivity in the first and second layers (n_1 and n_2) all describe soil hydrological properties.

Information about the saturated hydraulic conductivity (k_s) and the exponent of the unsaturated hydraulic conductivity curve (n) can be derived from soil textural information (e.g., Cosby et al. 1984; Rawls et al. 1993), as was done in Nijssen et al. (2001). We identified these parameters as calibration parameters for several reasons. First, it is difficult to determine average soil properties over an area as large as a 2° × 2° grid cell (about 49.5 × 10^3 km^2 at the equator). For example, Meeson et al. (1995) reported in the documentation that accompanies the CD-ROMs released as part of the International Satellite Land Surface Climatology Project, that they needed to shift all soil hydraulic properties by one soil textural class in order to obtain realistic drainage patterns with their model. Determination of areal average soil hydraulic properties is especially difficult, because most functions linking soil hydraulic properties to soil textural properties are highly nonlinear. Second, soil depths are generally not well known over large areas. Although Dunne and Wilmott (1996) developed a global dataset of plant-available moisture at a 0.5°, which included an estimate of rooting depth, these root zone estimates are strongly linked to the specific vegetation database used in that study.

Furthermore, and most importantly, the soil moisture transport mechanism in the VIC model is quite simple, consisting of gravity drainage with the hydraulic conductivity in each layer a function of the soil moisture storage within that layer. We implemented the VIC model in such a way that the plant roots could draw water only from the top two soil layers and the baseflow was generated only from the third layer. Consequently, the flux of water from the second layer into the third layer determines how much baseflow will occur. The ARNO model routing parameters (see the appendix) only determine how quickly the water stored in the third layer is evacuated. The transport of water through the second

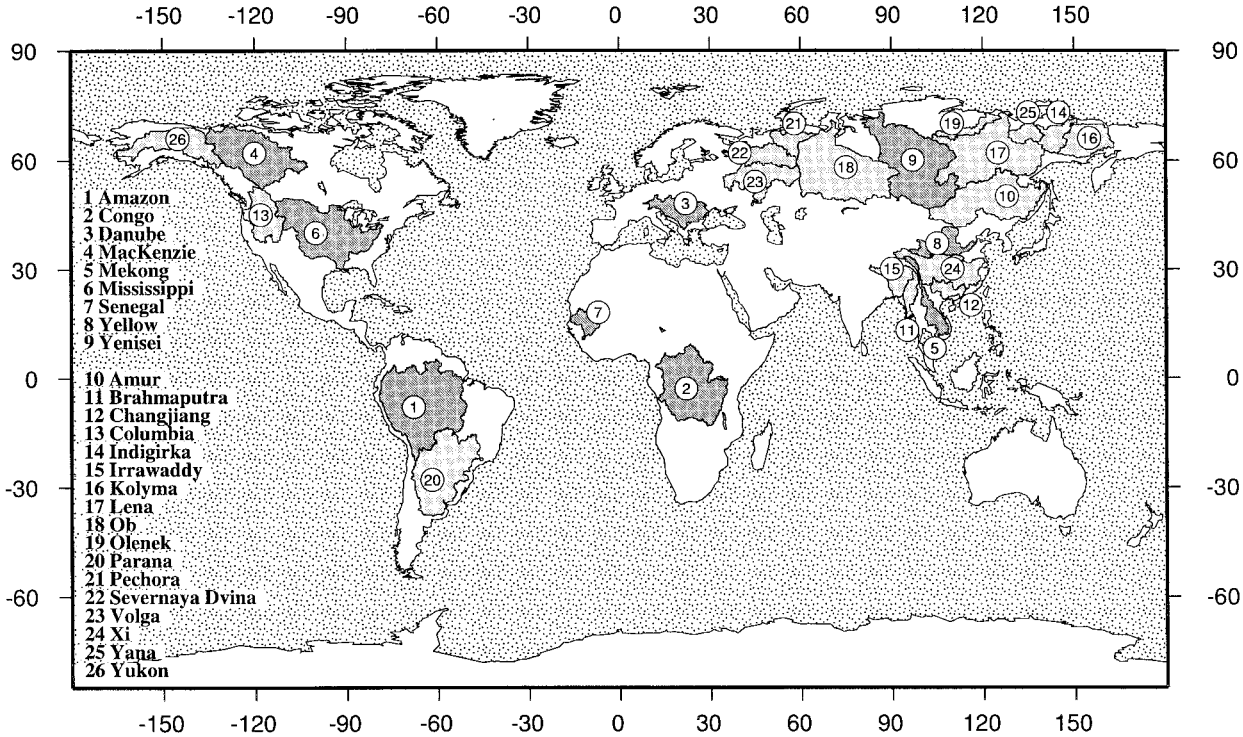

FIG. 2. Location of the 26 selected river basins. The nine dark-shaded basins form the primary group, and the light-shaded basins form the secondary group.

layer is largely determined by the parameters selected for calibration, because the VIC model calculates the hydraulic conductivity as

$$k = k_s\left(\frac{\theta}{\phi}\right)^n = k_s\left(\frac{W_n}{W_n^{\max}}\right)^n, \qquad (1)$$

with k the hydraulic conductivity, θ the moisture content, ϕ the porosity, W_n the moisture storage, and $W_n^{\max}$ the maximum moisture storage equal to ϕD, with D the depth of the layer. The moisture storage is dynamically determined by the model. A change in the thickness of the second layer affects not only the hydraulic conductivity, but also the maximum storage available in the second layer and consequently the water available for transpiration.

Climatic characteristics were selected as the basis for the transfer of calibration parameters under the premise that hydrological processes and the parameters used to describe them are more similar within than between different climate zones. To this end, each of the model grid cells was classified into one of five climatic zones (Table 2). These zones were constructed by regrouping the zones of the Köppen classification (e.g., Hubert et al. 1998).

An initial set of nine basins was selected for calibration on the basis of the following:

- the quality of the observed discharge record;
- the geographical location, to represent each climatic zone and continent, and
- the number of climate zones in each basin.

We tried to represent each climate zone and to have at least one basin on each continent. Australia was not represented, due to the high amount of regulation on the Australian rivers for which discharge data were available. To facilitate calibration and parameter transfer, the primary basins were selected to be located as much as possible within a single climate zone.

Calibration was performed manually and focused on matching the total annual flow volume and the shape of the mean monthly hydrograph. In the first round of calibration, all primary basins were grouped by climate zone and all basins within the same climate zone were calibrated using the same parameters. Although this approach was successful in the arctic and temperate climate zones, it did not work as well in the tropical climate zone. In particular, the calibrated parameters for the Amazon did not improve the model results for the Congo and vice versa. The tropical climate zone was therefore subdivided into three geographical regions: an American region from 180° to 30°W, an African region from 30°W to 60°E, and an Asian–Australian region from 60°E to 180°. It should be noted that the tropical climate zone encompasses all climates that are not defined as dry and where the mean daily maximum temperature is greater than 18°C in all months. However, this climate

TABLE 2. Grouping of Köppen climate zones into parameter transfer zones.

Parameter transfer zone	Köppen* climate zones	Climate characteristics**
1—Tropical	A	Tropical climate Not a B climate and $\overline{T_m} \geq 18°C$
2—Arid hot	Bh	Dry, warm climate B climate with $\overline{T_a} > 18°C$
3—Arid cold	Bk	Dry, cold climate B climate with $\overline{T_a} \leq 18°C$
4—Midlatitude rainy	C	Rainy, midlatitude climate Not a B climate and $-3°C < \overline{T_m}^{min} < 18°C$
	Da	Continental climate with hot summer Not a B climate and $\overline{T_m}^{min} < -3°C$ and $\overline{T_m}^{max} > 22°C$
	Db	Continental climate with cool summer Not a B climate and $\overline{T_m}^{min} < -3°C$ and $\overline{T_m}^{max} > 10°C$ for at least 4 months
5—Arctic	Dc	Continental climate with short cool summer Not a B climate and $\overline{T_m}^{min} < -3°C$ and $\overline{T_m}^{max} > 10°C$ for less than 4 months
	E	Polar climate Not a B climate and $\overline{T_m}^{max} < 10°C$

* Here B climates are defined as those climates for which $\overline{P_a} > 20\overline{T_a} + 140$ for those climates with equidistributed precipitation, $\overline{P_a} > 20\overline{T_a}$ when 70% of the annual precipitation falls in the coldest season, and $\overline{P_a} > 20\overline{T_a} + 280$ when 70% of the annual precipitation falls in the warmest season.

** Here $\overline{T}$ is the temperature (°C), $\overline{P}$ is the precipitation (mm), the subscripts m and a are used to indicate the monthly or annual period, and the superscripts min and max indicate the coldest and warmest months.

zone includes a number of different precipitation regimes. For instance, the Amazon basin is much wetter than the Congo basin, while the precipitation in Southeast Asia is monsoon dominated.

During the calibration process, the infiltration parameter (b_i) and the thickness of the second soil layer (D_2), which were treated as the primary calibration parameters, were changed to a uniform value in a given climate zone. For example, all grid cells in the American tropical zone were given the same b_i and D_2. The outer calibration parameters, which were used to fine tune the calibration, were changed from their original, spatially varying values using a regionally uniform multiplier. Consequently, after calibration the texture-based soil hydraulic parameters (k_s and n) varied spatially, while b_i and D_2 were constant within each region.

Generally, the thickness of the second soil layer was increased to allow for more storage. Only in the arctic climate zone was the thickness of the second soil layer reduced to 0.5 m. The unsaturated hydraulic conductivity and its exponent were changed to reduce the soil moisture flux in the arid climates, and to increase the soil moisture flux in the other climate zones. The calibrated infiltration parameter (b_i) tended to be smallest in the arid climates, in an effort to reduce runoff production.

Parameters were transferred from the primary to the secondary basins based on climate zone. For example, arctic cells in a secondary basin were modeled using parameters from the arctic zone, while temperate cells were modeled using parameters from the temperate zone. This meant that b_i and D_2 were set to the value for the climate zone, and that the soil hydraulic properties were modified by the multiplier for that zone.

To evaluate the effectiveness of the parameter transfer process and to provide the best possible global water balance estimates, the secondary basins were then further calibrated before transferring the parameters from all of the calibrated basins to the remaining global land surface grid cells. This second calibration was also performed by climate zone, although the primary basins were not modified. After this second calibration parameters were transferred to the rest of the global land surface area using the nearest calibrated grid cell within the same climate zone.

6. Results

a. Primary basins

Figure 3 shows the mean monthly hydrographs for the nine primary basins. The uncalibrated or base case simulation results are based on Nijssen et al. (2001). By construct, calibration improved the results in all instances, although in some cases the final calibration was still unsatisfactory, especially for arid basins such as the Senegal (Table 3). Some of these problems are related to the adopted routing scheme (section 4), since water is ''removed'' from the hydrologic cycle once it enters the stream channel. In addition, the Senegal flows through a region with strong precipitation gradients, which are not well resolved by the 2° × 2° forcing dataset. Further, the VIC model does not represent capillary rise in the soil zone. Although this process is usually of minor importance to the water budget in hu-

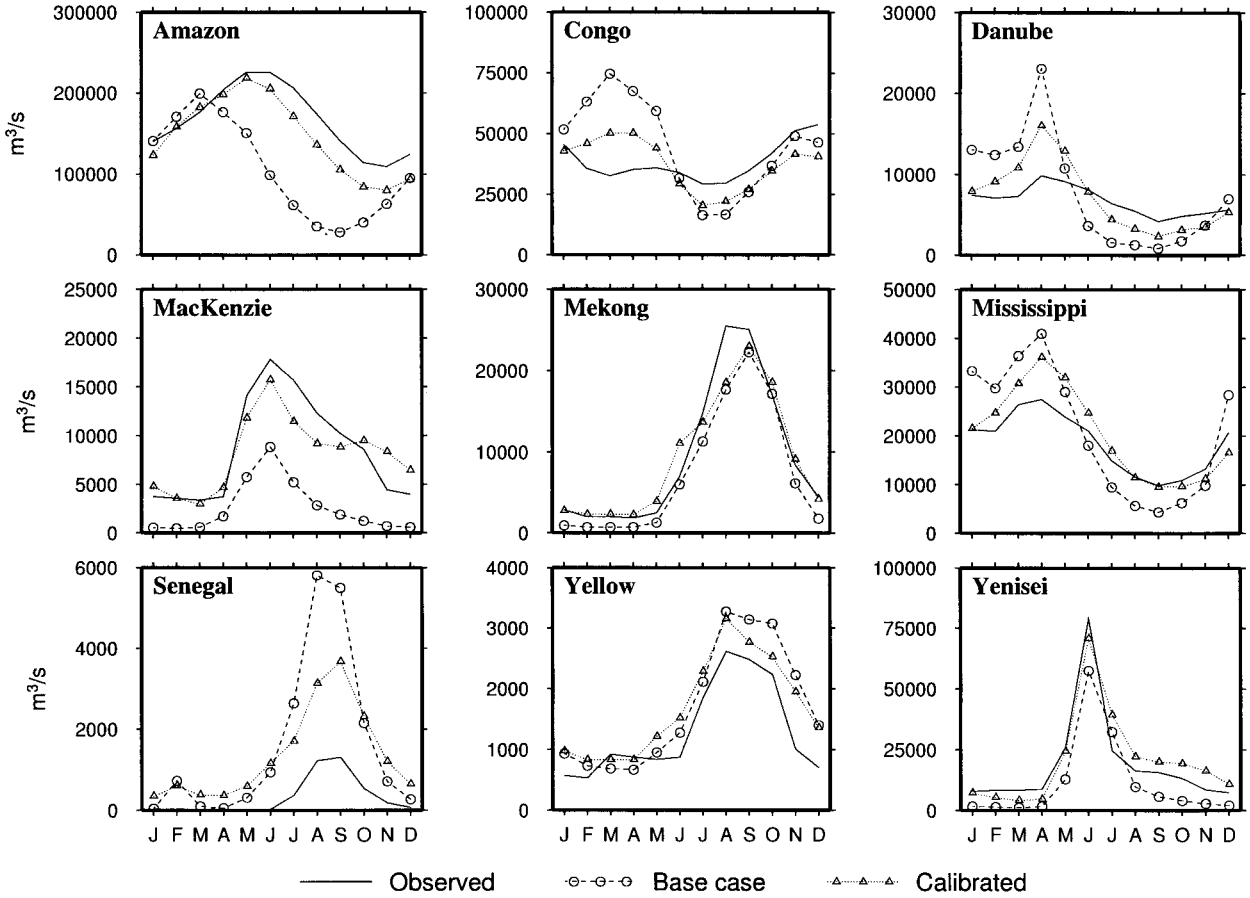

FIG. 3. Mean monthly hydrographs of observed and simulated flow (base case and calibrated) for the primary river basins.

mid areas, it may be significant in arid and semiarid regions. Excluding the Senegal, calibration reduced the mean bias from 28.9% to 9.9% and the relative root-mean-square error (rrmse) from 62.0% to 37.2%.

Figure 4 shows the annual runoff volumes as well as the annual precipitation for each of the basins. Although the changes in annual runoff volume between the base case and calibrated run are sometimes small (e.g., Mississippi and Danube), the calibrated model runs generally reflect the seasonal runoff cycle considerably better (Fig. 3). Except for the Congo River, the calibrated hydrographs peak within a month of the observed peak.

b. Secondary basins

Figures 5 and 6 are similar to Figs. 3 and 4, respectively, and show the parameter transfer and calibration results for the 17 secondary basins. Four of the 17 basins were excluded from the dataset after further examination revealed serious problems with the precipitation forcings. These four basins, the Yukon, Columbia, Brahmaputra, and Irrawaddy, are further discussed in section 7. Unfortunately, most of the remaining basins are in the northern mid- to high latitudes, which makes it difficult to evaluate the performance of the parameter transfer scheme for climate zones 1 and 2 (Table 2).

For the remaining 13 basins, the parameter transfer process improved the simulated flow volume in six cases (Amur, Indigirka, Kolyma, Lena, Olenek, and Yana), resulted in little or no change in three cases (Xi, Changjiang, and Volga) and resulted in a worse simulation in four cases (Paraná, Ob, Pechora, and Severnaya Dvina). Three of these last four basins are located in the western part of the Russian Arctic (from west to east of the Severnaya Dvina, Pechora, and Ob) and they differ from the basins immediately to the east in that their annual average precipitation is considerably higher. Whereas these three basins have a mean annual precipitation of about 600–800 mm, the basins to the east (such as the Yenisei and Lena) are much drier, with mean annual precipitation of about 400–500 mm. In the second round of calibration, these three basins were grouped and calibrated using a common set of parameters. For these three basins b_i was set to 0.25, the depth of the second soil layer to 2.5 m, and the hydraulic conductivities and exponents were reset to their precalibration values. This resulted in much improved flow volumes in all three cases. The depth of the second layer is unrealistic, but

TABLE 3. Calibration and parameter transfer statistics.

River basin	Base case		Parameter transfer		Calibration		
	Rrmse (%)[b]	Bias (%)[c]	Rrmse (%)[b]	Bias (%)[c]	Rrmse (%)[b]	Bias (%)[c]	n[a]
			Category 1				
Amazon	55.4	−39.8	—	—	24.1	−15.9	168
Congo	62.1	5.2	—	—	37.2	−13.1	113
Danube	85.3	12.3	—	—	42.2	5.1	60
MacKenzie	78.2	−69.0	—	—	31.7	−1.6	156
Mekong	42.6	−19.1	—	—	41.3	4.4	96
Mississippi	52.7	18.0	—	—	31.7	15.0	168
Senegal	712.6	424.3	—	—	431.2	340.2	60
Yellow	57.9	23.3	—	—	48.3	22.0	108
Yenisei	61.6	−44.4	—	—	41.1	2.2	168
			Category 2				
Amur	83.0	−45.9	41.1	−4.8	41.1	−4.8	132
Brahmaputra	61.1	−43.9	64.7	−46.2	—[d]	—[d]	84
Changjiang	32.5	−14.3	28.5	−14.1	28.4	11.2	84
Columbia	95.7	−74.3	88.2	−66.0	—[d]	—[d]	117
Indigirka	111.8	−54.7	75.7	−0.9	75.7	−0.9	165
Irrawaddy	72.0	−59.2	74.4	−60.7	—[d]	—[d]	108
Kolyma	99.9	−32.0	86.8	20.6	86.8	20.6	108
Lena	104.4	−68.2	60.6	−12.3	60.6	−12.3	168
Ob	250.5	46.5	222.6	101.7	93.7	4.7	168
Olenek	108.1	−36.7	82.7	24.3	85.9	17.0	60
Paraná	63.9	6.2	86.8	52.2	44.0	6.0	122
Pechora	85.1	16.3	87.1	41.3	60.2	14.0	108
Severnaya Dvina	132.2	31.3	143.8	79.0	62.3	8.2	165
Volga	320.9	83.6	204.7	86.1	138.1	21.1	60
Xi	42.2	−17.1	43.6	−15.8	43.6	−15.8	60
Yana	136.0	−74.6	87.3	13.0	87.3	13.0	60
Yukon	214.9	104.8	248.4	150.4	—[d]	—[d]	60

[a] Number of coincident months.
[b] Rrmse—relative root-mean-square error, defined as rrmse = $[1/n \sqrt{\Sigma_{i=1}^{n} (Q_{s,i} - Q_{o,i})^2}/\bar{Q}_o] \times 100\%$, with $Q_{s,i}$ and $Q_{o,i}$ the simulated and observed flow in month i.
[c] The bias, defined as bias = $[(\bar{Q}_s - \bar{Q}_o)/\bar{Q}_o] \times 100\%$.
[d] Excluded from further calibration and analysis because of problems with the precipitation forcings (section 7).

at present the VIC model does not allow for surface depression storage, which plays an important role immediately after snowmelt when the ground is still partially frozen in these cold climate basins. The deep soil layer acts partially as a surrogate for this surface storage.

Overall, parameter transfer reduced the rrmse from 120.8% to 96.3% and the mean bias from 40.6% to 35.9%. Further calibration of these basins reduced the rrmse to 69.8% and the bias to 11.5%. Four of the arctic basins (Indigirka, Kolyma, Lena, Yana) as well as the Amur and the Xi were not further calibrated in the second round, since the model results based on the parameter transfer were deemed sufficient.

c. *Continental water balance*

The calibrated parameters from the 22 calibrated basins were transferred to the rest of the globe, based on a nearest neighbor search within the same climate zone. The resulting continental water balances, summarized in Table 4, generally show an increase in runoff and, consequently, a decrease in evaporation compared with the base case simulation.

Globally, annual runoff increased 23 mm (9.4%) and evapotranspiration decreased 24 mm (5.0%). Because long-term storage changes are close to zero, the absolute change in runoff and evapotranspiration are about equal, but of opposite sign. The greatest decrease in evapotranspiration is in South America, where the modeled, annual evapotranspiration decreased by 119 mm (11.9%) and runoff increased 26.2% (119 mm). The runoff estimates are close to observation-based estimates from Lvovitch (1973) and Baumgartner and Reichel (1975) (Table 4), which is not surprising, because the calibration process ensured that the simulated runoff volumes are close to the observations. Table 4 clearly shows the large spread in continental precipitation and evapotranspiration estimates. The differences in evapotranspiration estimates largely stem from differences in the precipitation estimates. Although we have used recent global precipitation estimates in the construction of our model forcing dataset (Nijssen et al. 2001), the next section discusses some remaining problems.

7. Precipitation forcings

The precipitation dataset (Nijssen et al. 2001) was constructed on a 2° × 2° grid combining station obser-

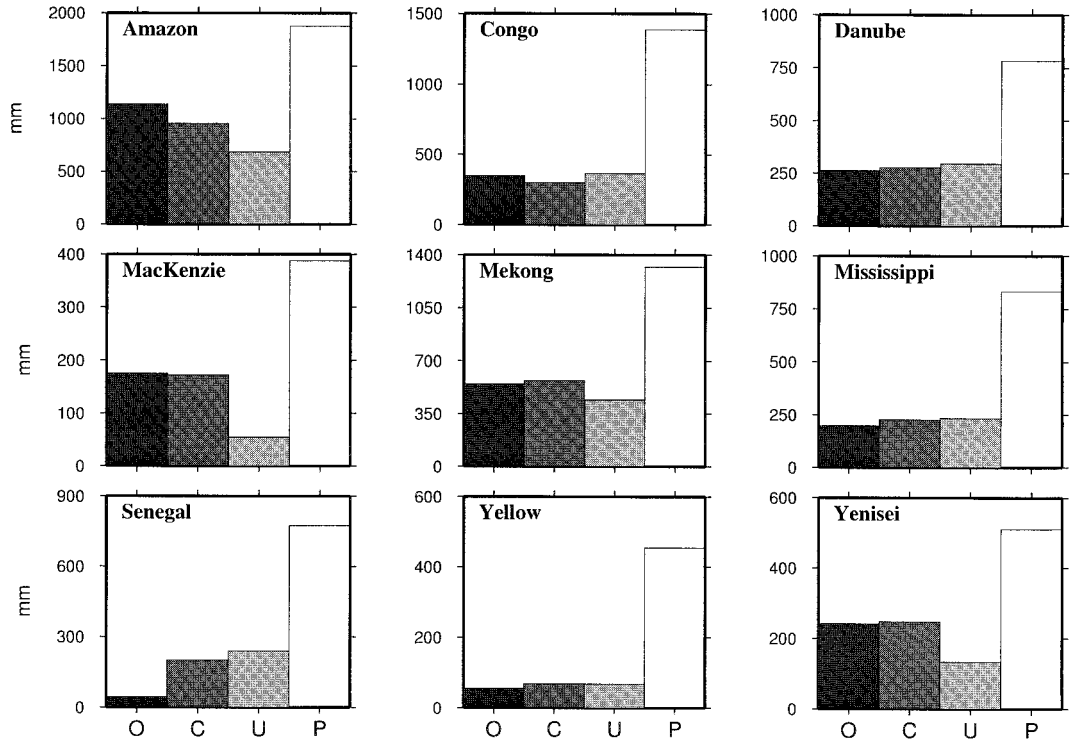

FIG. 4. Mean annual runoff [observed (O), calibrated (C), and base case (U)] and precipitation (P) for the primary river basins normalized by area. (Note that the observed runoff was normalized by the upstream area at the gauge as reported by GRDC or RivDis, and the simulated flow was normalized by the model area.)

vations with the monthly precipitation values from the 2.5° × 2.5° Global Precipitation Climatology Project (GPCP); (Huffman et al. 1997) and the 3.75° × 2.5° dataset from Hulme (1995). By construct, the monthly precipitation totals are the same as the monthly GPCP precipitation time series for the period covered by the GPCP dataset (1987 onward).

As mentioned earlier, it became apparent that the precipitation forcings at 2° × 2° resolution were suspect for four of the basins. For example, the mean annual precipitation over the Brahmaputra basin is 1144 mm, while the observed mean annual runoff is about 1133 mm for the same period (Fig. 6). If we assume that the long-term changes in terrestrial water storage are close to zero, this would leave only 10 mm yr^{-1} for evapotranspiration, which is clearly unrealistic. The Brahmaputra flows through the foothills of the Himalaya, where orographic effects result in high precipitation during the monsoon season. Clearly, the precipitation is underestimated. Consequently, our simulations result in modeled streamflow that is much lower than the observed streamflow. The same pattern, in even more extreme form, is observed for the Irrawaddy in Southeast Asia (mean annual precipitation of 900 mm and observed annual streamflow of 2203 mm for the area upstream of the gauge at Sagaing, Myanmar) and in somewhat less extreme form for the Columbia River in North America.

For some rivers the opposite effect was observed. For the Yukon River in North America the observed annual flow is about 159 mm, while the mean annual precipitation is about 627 mm. This would mean that the annual evapotranspiration in that region would be about 468 mm, which seems high given the short growing season and the long, cold winters. Consequently, our model results overestimated the mean annual streamflow in the Yukon. The high precipitation was largely due to model grid cells along the Gulf of Alaska, where a few stations, on which the GPCP climatology is based, show very high precipitation amounts (in excess of 2000 mm yr^{-1}).

To further diagnose problems with the precipitation forcings, the Columbia River simulation was evaluated in more detail. The Columbia River has been extensively studied with the VIC model at high spatial resolutions (0.25°, Matheussen et al. 2000 and 0.125°, Hamlet and Lettenmaier 1999) and good estimates of precipitation are available for this area. Figure 7 shows the mean annual precipitation over the Columbia River basin for the 2° × 2° resolution global dataset (based on the GPCP dataset), and a regional climatology produced by Daly et al. (1994) aggregated to 0.125° and 2°. The Parameter-elevation Regressions on Independent Slopes Model (PRISM) developed by Daly et al. (1994) produces a precipitation climatology at a resolution of 2.5 min, based on more than 8000 precipitation stations over the

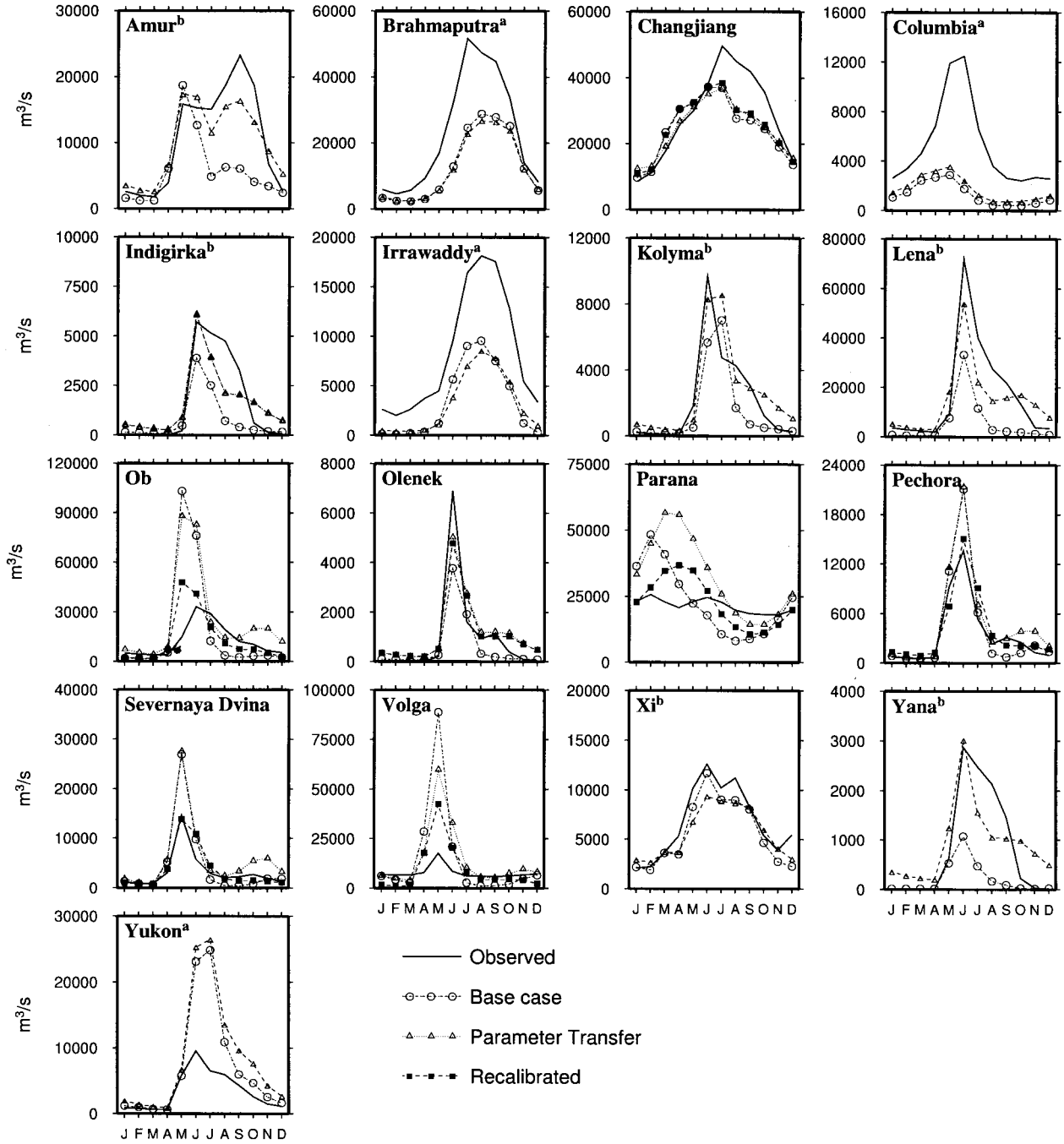

FIG. 5. Mean monthly hydrographs of observed and simulated flow (base case, parameter transfer, and recalibrated) for the secondary river basins. [a]Basins excluded from further analysis because of problems with the precipitation forcing. [b]Basins that were not further calibrated after the parameter transfer, because the hydrograph and flow volume were considered adequate.

continental United States. Its distinguishing feature is that it accounts for orographic effects by calculating local regression relationships between precipitation and elevation, and using these relationships to estimate mean areal precipitation. Whereas the GPCP-based precipitation generally decreases from west to east over the Columbia River basin, the PRISM-based precipitation shows a much more complex spatial pattern with the highest precipitation along the northwestern (Cascade Mountains), and the northern and eastern (Rocky Mountains) perimeters of the basin.

To further diagnose whether the undersimulation of streamflow in the Columbia River was due to the precipitation or to a poor combination of parameters, we

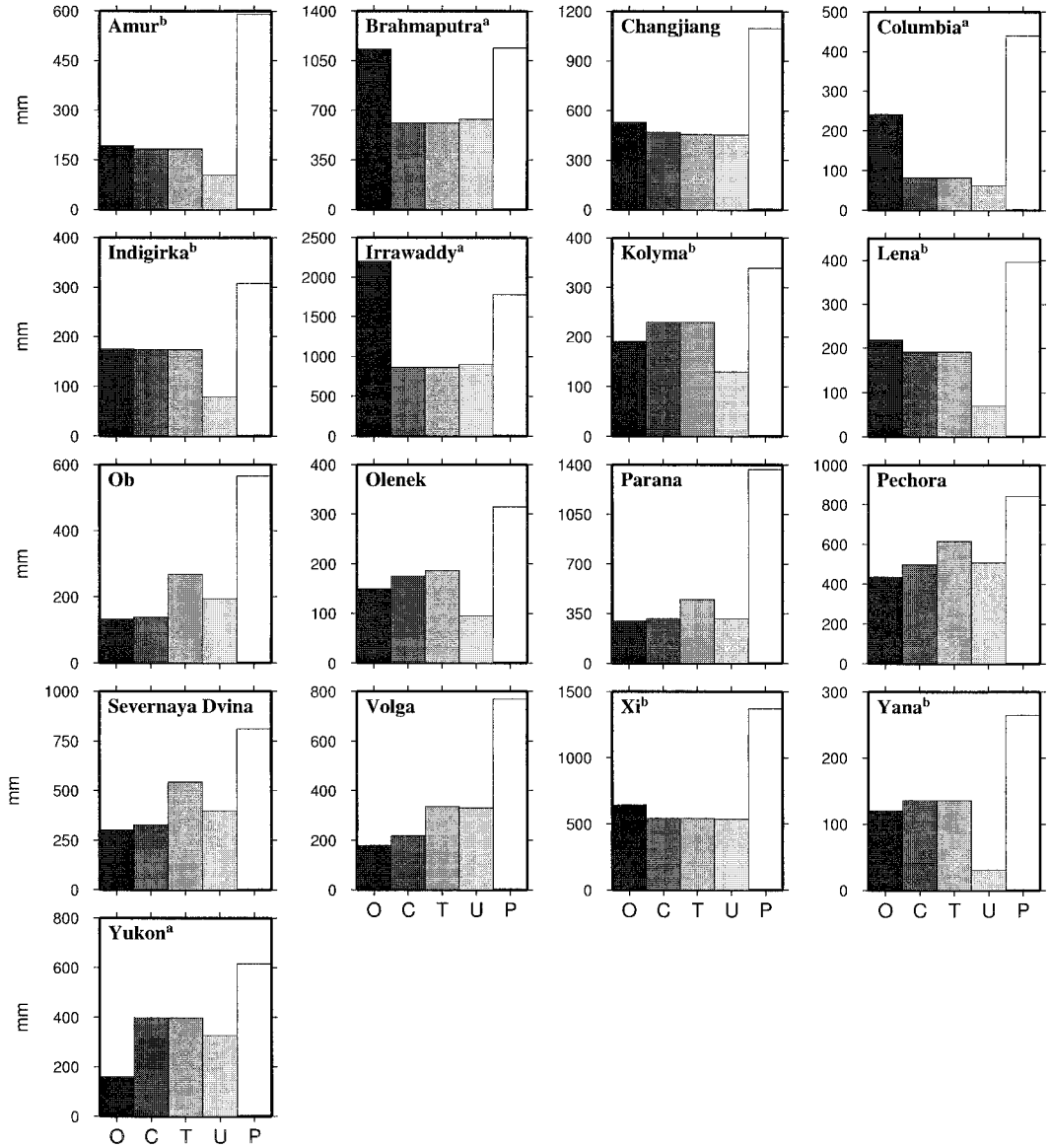

FIG. 6. Mean annual runoff [observed (O), calibrated (C), parameter transfer (T), and base case (U)] and precipitation (P) for the secondary river basins normalized by area (see Fig. 4 for note on normalization). [a]Basins excluded from further analysis, because of problems with the precipitation forcing. [b]Basins that were not further calibrated after the parameter transfer, because the hydrograph and flow volume were considered adequate.

forced the VIC model with the PRISM-based precipitation aggregated to 2° × 2°. Additionally, we used a station-based temperature dataset (Hamlet and Lettenmaier 1999) to ensure that biases in the temperature were not the cause for the poor simulation results. Figure 8 shows the observed Columbia River hydrograph, and the results from four separate model runs. Note that the ''observed'' flows have been adjusted to account for the effects of reservoir regulation, that is, they are the flows that would have occurred in the absence of reservoirs or other water management effects (A. G. Crook Company 1993). The first model run uses the forcing data used in this study. The second model run uses the same precipitation, with the station-based temperature data from Hamlet and Lettenmaier (1999). The third model run uses the same temperature data as the first run, but uses the PRISM-based precipitation, aggregated to 2° spatial resolution. The fourth model run uses the station-based temperature data from Hamlet and Lettenmaier (1999) and the PRISM precipitation. All other model parameters are identical for each of the four runs. The figure demonstrates clearly that the modeled streamflow is highly sensitive to the quality of the precipitation estimates. If the high-resolution PRISM dataset, which includes the effects of orography on precipitation, is taken as the ''true'' precipitation, the model results are

TABLE 4. Annual continental water balance (P—precipitation, E—evapotranspiration, R—runoff). Continents are defined according to Oki et al. (1995). Europe includes Turkey and extends as far east as the Urals. Australia includes New Zealand and New Guinea. All estimates except for Oki et al. (1995) are based on hydrological methods. The estimate from Oki et al. (1995) is based on atmospheric water balance computations using global analysis data from the European Centre for Medium-Range Weather Forecasts.

Variable	All lands	Asia	Europe	Africa	North America	South America	Australia	Reference
P	727	590	769	655	633	1449	680	
E	459	330	484	536	375	876	486	This study
R	267	259	280	121	256	573	193	
P	727	590	769	655	633	1449	680	
E	483	366	436	511	409	995	485	Nijssen et al. (2001)
R	244	224	333	145	222	454	193	
P	834	726	734	686	670	1648	736	
E	540	433	415	547	383	1065	510	Lvovitch (1973)
R	294	293	319	139	287	583	226	
P		515	593	728	738	1440	495*	
E		346	328	525	423	990	418*	Kalinin (1971)
R		169	265	203	315	450	77*	
P	746	696	657	696	645	1564	803/447**	
E	480	420	375	582	403	946	534/420**	Baumgartner and Reichel (1975)
R	266	276	282	114	242	618	269/27**	
P − E = R	303	300	273	153	315	678	278	Korzun (1978)
P − E = R	165	235	136	−100	263	415	54	Oki et al. (1995)

* The definition of Australia used by Kalinin (1971) does not include New Zealand or New Guinea.
** The first value includes the islands in Oceania and much of the Pacific; the second value refers to the mainland of Australia only.

comparable to those for the other basins and the parameter transfer could have been regarded as moderately successful. However, using the GPCP-based precipitation, the streamflow is severely underpredicted.

Unlike the Columbia River basin, the two precipitation datasets agreed reasonably well with respect to the mean annual precipitation over the Mississippi River basin and the mean annual simulated streamflow was within 15% of the observed flow. In the Mississippi basin, the effects of the orography are largely limited to grid cells along the northwestern edge of the basin (Rocky Mountains).

Generally it appears that the greatest weakness of the precipitation dataset is in areas with complex topography, such as coastal mountain ranges, where very strong gradients in precipitation exist. In these areas, the small number of stations per grid cell used in the construction of the GPCP dataset do not adequately reflect the areal average precipitation. In addition, the relatively coarse modeling grid can lead to erroneous precipitation forcings when, for example, a river drains the lee side of a mountain range. If the mountain range is narrow, the coarse-resolution precipitation data includes precipitation from the windward side of the mountain range, resulting in an overprediction of the total precipitation input. Because of the problems with the precipitation inputs, the four rivers mentioned earlier in this section were not further calibrated and their parameters were excluded from the nearest neighbor search in the parameter transfer process.

8. Conclusions

The ability to represent runoff and streamflow from large river basins, and from continents in total, is critical to an understanding of the global hydrologic cycle. Streamflow is important not only for water resource studies, but it is also the most commonly available component of the surface water balance, and therefore can be used in a variety of diagnostic studies (e.g., Maurer et al. 2001). The runoff formulation in most MHMs is quasi-conceptual, which necessitates some calibration of model parameters. We found that calibration of a restricted number of VIC model parameters reduced the relative root-mean-square error (rrmse) of the monthly flows from 62% to 37% and the mean bias in annual flows from 29% to 10%. Problems in model predictions remain in hot, arid areas, where the VIC model tends to overestimate the mean annual runoff.

However, calibration is a time-consuming process and quickly becomes infeasible when the model area or the number of basins increases. Therefore, a methodology of model parameter transfer was developed to limit the number of basins for which calibration was needed. As a first attempt, model cells were grouped by climate zone, and model parameters were transferred within these groups. Although, the results were mixed, the transferred parameters reduced the rrmse from 121% to 96% and the mean bias from 41% to 36%. Further calibration of these basins reduced the rrmse to 70% and the bias to 12%.

After the parameter transfer from all calibrated basins to the rest of the globe, the mean annual global runoff increased 9.4% and the evapotranspiration decreased 5.0% relative to the values reported by Nijssen et al. (2001) for a model run without calibration. However, on a continental basis the changes were much larger. For South America, the simulated evapotranspiration was 119 mm (12%) smaller than in the base case sce-

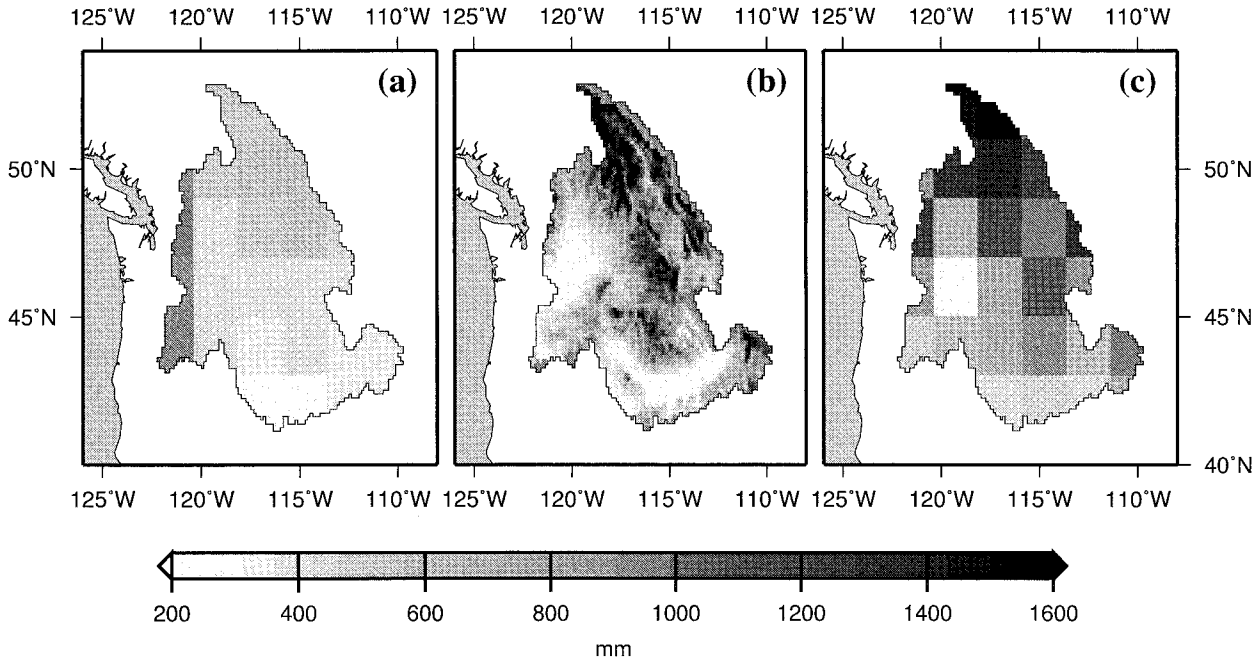

FIG. 7. Mean annual precipitation over the Columbia River basin in western North America: (a) GPCP-based precipitation at 2° × 2°; (b) PRISM-based precipitation at 0.125° × 0.125°; (c) PRISM-based precipitation at 2° × 2°.

nario. This corresponds to a decrease in the mean latent heat flux of 9.4 W m^{-2}. Because evapotranspiration shows a strong diurnal cycle, the maximum instantaneous change in the latent heat flux is much larger.

Our study also pointed out some shortcomings in the global datasets used. Lack of available streamflow observations as well as regulation on many of the world's largest rivers halved the number of rivers in our original dataset. There is a great need for recent (post 1980) streamflow data for these rivers. Difficulties with the precipitation forcing eliminated an additional four river basins. Some of the precipitation problems were due to

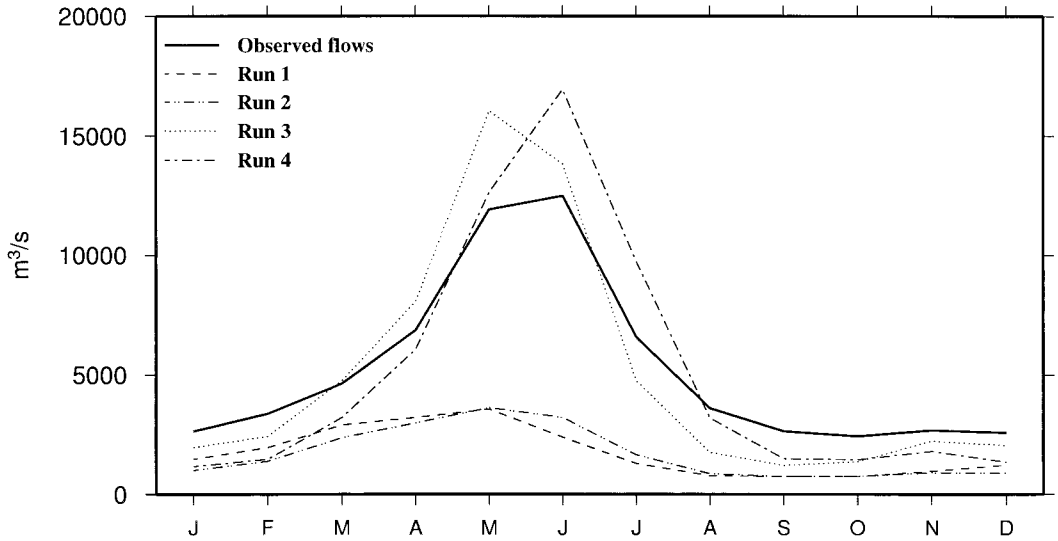

FIG. 8. Mean monthly observed and simulated hydrograph for the Columbia River. The simulations are based on four different combinations of precipitation and temperature datasets. Run 1: precipitation and temperature data as used in this study. Run 2: precipitation as used in this study and temperature from Hamlet and Lettenmaier (1999). Run 3: PRISM-based precipitation and temperature as used in this study. Run 4: precipitation and temperature from Hamlet and Lettenmaier (1999). See text for details.

the coarse resolution of the GPCP-based dataset (2° × 2°), which failed to resolve strong spatial gradients in the precipitation. However, a more persistent problem was the underestimation of the precipitation in areas with complex terrain. Because most precipitation stations in those areas tend to be located in areas with low elevation, the effects of orographic enhancement are not adequately represented. Comparison of the mean annual precipitation field over the Columbia River basin with a PRISM-based precipitation field showed that the annual biases could be as large as 1000 mm.

The parameter transfer method resulted in only a modest improvement in the streamflow simulations. It is clear from these early results that many questions remain. What are the best criteria for grouping basins or grid cells? How can parameters be transferred within and between these groups? Which parameters can safely and successfully be transferred? However, despite these difficulties, we think that the parameter transfer process is one of the few realistic options for performing large-scale or global hydrological simulations.

Both the meteorological forcing dataset and the model-simulated water balance components are available to the scientific community through the World Wide Web (information is available online at http://www.hydro.washington.edu).

Acknowledgments. Dr. Qingyun Duan (U.S. National Weather Service) and Dr. Hoshin Gupta (University of Arizona) provided the shuffled complex evolution (SCE) code and graciously answered our questions regarding application of the algorithm. The Bonneville Power Administration provided the modified flows for the Columbia River. This work was supported by the U.S. Environmental Protection Agency under STAR Grant R 824802-01-0 to the University of Washington.

APPENDIX

ARNO Baseflow Formulation

The ARNO baseflow parameterization represents drainage from the lower soil layer as a function of the soil moisture content of that layer (Todini 1996). Outflow is modeled using a linear reservoir when the moisture content is low, and a nonlinear reservoir when it is high (Lohmann et al. 1998a). The ARNO baseflow model can be written as

$$Q_b = \begin{cases} d_1 W_n, & 0 \le W_n \le d_3, \\ d_1 W_n + d_2 (W_n - d_3)^{d_4}, & d_3 < W_n \le W_n^{\max}, \end{cases} \tag{A1}$$

where Q_b is the daily baseflow discharge, W_n is the soil moisture content, d_1 is a linear reservoir coefficient, d_2 is a nonlinear reservoir coefficient, d_3 is the soil moisture level at which the baseflow transitions from linear to nonlinear, and d_4 is the exponent of the nonlinear part of the outflow curve (note that $d_4 \ge 1$).

Todini (1996) suggests that although the values of these baseflow parameters cannot be obtained directly through observation, they can be obtained through calibration and ". . . they tend to be easily identified on long recession periods and by matching the overall mass balance. . ." [note that the parameters are defined differently in Todini (1996), but that the functional form of the equations is the same]. Obviously, such a calibration approach is not viable for a global application because of the large number of locations for which separate calibrations would be needed. Instead, we were able to derive an initial set of baseflow parameters for selected river basins directly from the observed hydrographs using a modified version of the method described by Abdulla et al. (1999).

We selected 502 basins around the world from the GRDC river discharge database for purposes of estimating baseflow parameters. Only relatively small basins (drainage areas between 100 and 50 000 km^2) were used to minimize in-channel flow routing effects on the shape of the hydrographs. Stations were selected based on the period of coverage, the quality of the data record, and geographical location. For certain areas of the globe it was difficult to obtain hydrograph series of reasonable length and quality, and some of the final stations had records of relatively short duration and/or many missing values.

Baseflow sequences were defined as those periods during which the observed discharge declined monotonically for a period of 5 or more days. As an additional requirement only flows smaller than the 90th percentile were considered in order to avoid including the highest flows, which are likely to include a relatively large "fast" response component. Fifty-eight out of 502 stations did not have a baseflow sequence that met these requirements.

The linear reservoir coefficient d_1 was determined by regression of the scaled discharge $\ln Q_b^n/Q_b^o$ against time t_n, where Q_b^o is the first discharge value in the baseflow series, Q_b^n the discharge on day t_n, and t_n is the number of days since the start of the baseflow series. Only flows smaller than the 50th-percentile flow were considered to be generated by the linear baseflow mechanism. A further 100 stations did not have sufficient data to calculate d_1, leaving a total of 347 stations for which d_1 was estimated.

The remaining baseflow parameters (d_2, d_3, and d_4) were obtained by fitting (A1) to all baseflow sequences through optimization using the shuffled complex evolution (SCE) algorithm (Duan et al. 1992, 1993, 1994). As suggested by Abdulla et al. (1999), the optimum parameter values were determined by ordinary least squares applied to transformed (Box–Cox), prewhitened residuals. The Box–Cox transformation parameter λ was included as one of the optimized variables.

The resulting 347 baseflow parameter sets were in-

terpolated to the individual 2° × 2° grid cells using a moving window with a radius of 250 km. If more than one baseflow parameter set was available within 250 km from the center of the grid cell, the baseflow parameter values were averaged, otherwise the nearest baseflow parameter set was used.

REFERENCES

Abdulla, F. A., and D. P. Lettenmaier. 1997a: Application of regional parameter estimation schemes to simulate the water balance of a large continental river. *J. Hydrol.,* **197,** 258–285.

——, and ——, 1997b: Development of regional parameter estimation equations for a macroscale hydrologic model. *J. Hydrol.,* **197,** 230–257.

——, ——, E. F. Wood, and J. A. Smith, 1996: Application of a macroscale hydrologic model to estimate the water balance of the Arkansas–Red River Basin. *J. Geophys. Res.,* **101,** 7449–7459.

——, ——, and X. Liang, 1999: Estimation of the ARNO model baseflow parameters using daily streamflow data. *J. Hydrol.,* **222,** 37–54.

A. G. Crook Company, 1993: 1990 level modified streamflow 1928–1989. Bonneville Power Administration Tech. Rep., Contract DE-AC79-92BP21985, 280 pp. [Available from Bonneville Power Administration, P.O. Box 3621, Portland, OR 97208.]

Batjes, N. H., 1995: A homogenized soil data file for global environmental research: A subset of FAO, ISRIC and NCRS profiles. International Soil Reference and Information Centre (ISRIC) Tech. Rep. 95/10, 50 pp. [Available from ISRIC, P.O. Box 535, 6700AJ Wageningen, Netherlands.]

Baumgartner, A., and E. Reichel, 1975: *The World Water Balance: Mean Annual Global, Continental and Maritime Precipitation, Evaporation and Runoff*. Elsevier Scientific, 179 pp.

Bowling, L. C., D. Lettenmaier, and B. V. P. Matheussen, 2000: Hydroclimatology of the arctic drainage basin. *The Freshwater Budget of the Arctic Ocean.* E. L. Lewis et al., Eds., NATO ARW, Kluwer Academic, 57–90.

Bras, R. A., 1990: *Hydrology, an Introduction to Hydrologic Science.* Addison Wesley, 643 pp.

Comanor K., B. Nijssen, and D. P. Lettenmaier, 2000: Comment on ''Five-minute, 1/2° and 1° data sets of continental watersheds and river networks for use in regional and global hydrologic and climate modeling studies'' by Graham et al. *Water Resour. Res.,* **36,** 3117–3120.

Cosby, B. J., G. M. Hornberger, R. B. Clapp, and T. R. Ginn, 1984: A statistical exploration of the relationships of soil mixture characteristics to the physical properties of soils. *Water Resour. Res.,* **20,** 682–690.

Daly, C., R. P. Neilson, and D. L. Phillips, 1994: A statistical–topographic model for mapping climatological precipitation over mountainous terrain. *J. Appl. Meteor.,* **33,** 140–158.

Duan, Q., S. Sorooshian, and V. K. Gupta, 1992: Effective and efficient global optimization for conceptual rainfall–runoff models. *Water Resour. Res.,* **28,** 1015–1031.

——, V. K. Gupta, and S. Sorooshian, 1993: Shuffled complex evolution approach for effective and efficient global minimization. *J. Optimization Theory Appl.,* **76,** 501–521.

——, S. Sorooshian, and V. K. Gupta, 1994: Optimal use of the SCE–UA global optimization method for calibrating watershed models. *J. Hydrol.,* **158,** 265–284.

Dümenil, L., and E. Todini, 1992: A rainfall–runoff scheme for use in the Hamburg climate model. *Adv. Theor. Hydrol.,* **9,** 129–157.

Dunne, K. A., and C. J. Wilmott, 1996: Global distribution of plant-extractable water capacity of soil. *Int. J. Climatol.,* **16,** 841–859.

FAO, 1995: The digital soil map of the world, Version 3.5. United Nations Food and Agriculture Organization, CD-ROM. [Available from Food and Agriculture Organization of the United Nations, Via delle Terme di Caracalla, 00100 Rome, Italy.]

Graham, S. T., J. S. Famiglietti, and D. R. Maidment, 1999: 5-minute, 1/2°, and 1° data sets of continental watersheds and river networks for use in regional and global hydrologic and climate system modeling studies. *Water Resour. Res.,* **35,** 583–587.

Hamlet, A. F., and D. P. Lettenmaier, 1999: Effects of climate change on hydrology and water resources in the Columbia River basin. *J. Amer. Water Resour. Assoc.,* **35,** 1597–1623.

Hansen, M. C., R. S. DeFries, J. R. G. Townshend, and R. Sohlberg, 2000: Global land cover classification at 1 km spatial resolution using a classification tree approach. *Int. J. Remote Sens.,* **21,** 1331–1364.

Hubert, B., L. François, P. Warnant, and D. Strivay, 1998: Stochastic generation of meteorological variables and effects on global models of water and carbon cycles in vegetation and soils. *J. Hydrol.,* **212–213,** 318–334.

Huffman, and Coauthors, 1997: The Global Precipitation Climatology Project (GPCP) combined precipitation dataset. *Bull. Amer. Meteor. Soc.,* **78,** 5–20.

Hulme, M., 1995: Estimating global changes in precipitation. *Weather,* **50,** 34–42.

Jones, P. D., 1994: Hemispheric surface air temperature variations: A reanalysis and an update to 1993. *J. Climate,* **7,** 1794–1802.

Kalinin, G. P., 1971: *Global Hydrology.* Israel Program for Scientific Translations, 312 pp. First published in *Problemy global'noi gidrologii,* Gidrometeorologicheskoe Izdatel'svo, 1968.

Kalnay, E., and Coauthors, 1996: The NCEP/NCAR 40-Year Reanalysis Project. *Bull. Amer. Meteor. Soc.,* **77,** 437–471.

Kimball, J. S., S. W. Running, and R. R. Nemani, 1997: An improved method for estimating surface humidity from daily minimum temperature. *Agric. For. Meteor.,* **85,** 87–98.

Kite, G., 1998: Land surface parameterizations of GCMs and macroscale hydrological models. *J. Amer. Water Resour. Assoc.,* **34,** 1247–1254.

Korzun, V. I., 1978: *World Water Balance and Water Resources of the World.* UNESCO Studies and Reports in Hydrology, Vol. 25, UNESCO, 663 pp.

Kuhl, S. C., and J. R. Miller, 1992: Seasonal river runoff calculated from a global atmospheric model. *Water Resour. Res.,* **28,** 2029–2039.

Leung, L. R., A. F. Hamlet, D. P. Lettenmaier, and A. Kumar, 1999: Simulations of the ENSO hydroclimate signals in the Pacific Northwest Columbia River Basin. *Bull. Amer. Meteor. Soc.,* **80,** 2313–2329.

Liang, X., D. P. Lettenmaier, E. F. Wood, and S. J. Burges, 1994: A simple hydrologically based model of land surface water and energy fluxes for general circulation models. *J. Geophys. Res.,* **99,** 14 415–14 428.

——, ——, and ——, 1996: One-dimensional statistical dynamic representation of subgrid spatial variability of precipitation in the two-layer variable infiltration capacity model. *J. Geophys. Res.,* **101,** 21 403–21 422.

——, and Coauthors, 1998: The Project for Intercomparison of Land-surface Parameterization Schemes (PILPS) Phase 2(c) Red–Arkansas River Basin experiment: 2. Spatial and temporal analysis of energy fluxes. *Global Planet. Change,* **19,** 137–159.

Linsley, R. K., M. A. Kohler, and J. L. H. Paulhus, 1986: *Hydrology for Engineers.* 3d ed. McGraw-Hill, 508 pp.

Liston, G. E., Y. C. Sud, and E. F. Wood, 1994: Evaluating GCM land surface hydrology parameterizations by computing river discharges using a runoff routing model. *J. Appl. Meteor.,* **33,** 394–405.

Lohmann, D., R. Nolte-Holube, and E. Raschke, 1996: A large-scale horizontal routing model to be coupled to land surface parameterization schemes. *Tellus,* **48A,** 708–721.

——, E. Raschke, B. Nijssen, and D. P. Lettenmaier, 1998a: Regional scale hydrology: I. Formulation of the VIC-2L model coupled to a routing model. *Hydrol. Sci. J.,* **43,** 131–141.

——, ——, ——, and ——, 1998b: Regional scale hydrology: II.

Application of the VIC-2L model to the Weser River, Germany. *Hydrol. Sci. J.,* **43,** 143–158.

——, and Coauthors, 1998c: The Project for Intercomparison of Land-surface Parameterization Schemes (PILPS) Phase 2(c) Red–Arkansas River Basin experiment: 3. Spatial and temporal analysis of water fluxes. *Global Planet. Change,* **20,** 161–179.

Lvovitch, M. I., 1973: The global water balance. *Eos, Trans. Amer. Geophys. Union,* **54,** 28–42.

Matheussen, B., R. L. Kirschbaum, I. A. Goodman, G. M. O'Donnell, and D. P. Lettenmaier, 2000: Effects of land cover change on streamflow in the interior Columbia River basin (USA and Canada). *Hydrol. Processes,* **14,** 867–885.

Maurer, E. P., G. M. O'Donnell, D. P. Lettenmaier, and J. O. Roads, 2001: Evaluation of NCEP/NCAR reanalysis water and energy budgets using macroscale hydrological simulations as a benchmark. *Land Surface Hydrology, Meteorology, and Climate: Observations and Modeling,* V. Lakshmi, J. Albertson, and J. Schaake, Eds., Vol. 3, *Water Science and Applications,* Amer. Geophys. Union, 137–158.

Meeson, B. W., F. E. Corprew, J. M. P. McManus, D. M. Myers, J. Closs, K. Sun, D. Sunday, and P. Sellers, 1995: ISLSCP initiative I—Global data sets for land–atmosphere models 1987–1988. Vols. 1–5, NASA, CD-ROM. [Available from Goddard DAAC Help Desk, Code 902.2, NASA Goddard Space Flight Center, Greenbelt, MD 20771.]

Miller, J. R., G. L. Russell, and G. Caliri, 1994: Continental-scale river flow in climate models. *J. Climate,* **7,** 914–928.

Nijssen, B., D. P. Lettenmaier, X. Liang, S. W. Wetzel, and E. F. Wood, 1997: Streamflow simulation for continental-scale river basins. *Water Resour. Res.,* **33,** 711–724.

——, R. Schnur, and D. P. Lettenmaier, 2001: Global restrospective estimation of soil moisture using the VIC land surface model, 1980–93. *J. Climate,* **14,** 1790–1808.

O'Donnell, G., B. Nijssen, and D. P. Lettenmaier, 1999: A simple algorithm for generating streamflow networks for grid-based, macroscale hydrological models. *Hydrol. Processes,* **13,** 1269–1275.

Oki, T., and Y. C. Sud, 1998: Design of Total Runoff Integrating Pathways (TRIP). *Earth Interactions,* **2,** 1–53. [Available online at http://earthinteractions.org.]

——, K. Musiake, H. Matsuyama, and K. Masuda, 1995: Global atmospheric water balance and runoff from large river basins. *Hydrol. Processes,* **9,** 655–678.

Rawls, W. J., L. R. Ahuja, D. L. Brakensiek, and A. Shirmohammadi, 1993: Infiltration and soil water movement. *Handbook of Hydrology,* D. R. Maidment, Ed., McGraw-Hill, 5.1–5.51.

Riverside Technologies, Inc., and Harza Engineering, 1994: *User's Guide to the Columbia River Forecast System.* Bonneville Power Administration, 78 pp.

Robock, A., C. A. Schlosser, K. Y. Vinnikov, N. A. Speranskaya, J. K. Entin, and S. Qiu, 1998: Evaluation of the AMIP soil moisture simulation. *Global Planet. Change,* **19,** 181–208.

——, K. Y. Vinnikov, G. Srinivasan, J. K. Entin, S. E. Hollinger, N. A. Speranskaya, S. Liu, and A. Namkhai, 2000: The global soil moisture data bank. *Bull. Amer. Meteor. Soc.,* **81,** 1281–1299.

Row, L. W., D. A. Hastings, and P. K. Dunbar, 1995: TerrainBase worldwide digital terrain data documentation manual, release 1.0. National Geophysical Data Center, CD-ROM. [Available online at http://www.ngdc.noaa.gov, or from National Geophysical Data Center, Mail Code E/GC, 325 Broadway, Boulder, CO 80303-3328.]

Russell, G. L., and J. R. Miller, 1990: Global river runoff calculated from a global atmosphere general circulation model. *J. Hydrol.,* **116,** 241–254.

Sausen, R., S. Schubert, and L. Dümenil, 1994: A model of river runoff for use in coupled atmosphere–ocean models. *J. Hydrol.,* **155,** 337–352.

Thornton, P. E., and S. W. Running, 1999: An improved algorithm for estimating incident daily solar radiation from measurements of temperature, humidity, and precipitation. *Agric. For. Meteor.,* **93,** 211–228.

Todini, E., 1996: The ARNO rainfall–runoff model. *J. Hydrol.,* **175,** 339–382.

Vörösmarty, C. J., K. P. Sharma, B. Fekete, A. H. Copeland, J. Holden, J. Marble, and J. A. Lough, 1997: The storage and aging of continental runoff in large reservoir systems of the world. *Ambio,* **26,** 210–217.

——, B. M. Fekete, and B. A. Tucker, cited 1998: Global River Discharge Database (RivDis) Version 1.1. [Available online at http://www-eosdis.ornl.gov.]

Wood, E. F., D. P. Lettenmaier, and V. G. Zartarian, 1992: A land-surface hydrology parameterization with subgrid variability for general circulation models. *J. Geophys. Res.,* **97,** 2717–2728.

——, ——, X. Liang, B. Nijssen, and S. W. Wetzel, 1997: Hydrological modeling of continental-scale basins. *Annu. Rev. Earth Planet. Sci.,* **25,** 279–300.

——, and Coauthors,1998: The Project for Intercomparison of Land-surface Parameterization Schemes (PILPS) Phase 2(c) Red–Arkansas River Basin experiment: 1. Experiment description and summary intercomparisons. *Global Planet. Change,* **19,** 115–135.

Zhao, R. J., Y. L. Zhang, L. R. Fang, and Q. S. Zhang, 1980: The Xinanjiang model. *Hydrological Forecasting, Proc. Oxford Symp. on Hydrological Forecasting,* Oxford, United Kingdom, IAHS, 351–356.